



# Study of grain boundary polarization by two-probe and four-probe impedance spectroscopy

J.R. Dygas<sup>a,\*</sup>, G. Faflek<sup>b</sup>, M.W. Breiter<sup>b</sup>

<sup>a</sup>*Instytut Fizyki, Politechnika Warszawska, Chodkiewiczza 8, 02-524 Warsaw, Poland*

<sup>b</sup>*Institut für Technische Elektrochemie, TU Wien, Getreidemarkt 9/158, A-1060 Vienna, Austria*

---

## Abstract

Four-probe impedance spectra of polycrystalline cation conductors: NASICON, Na  $\beta$ '-alumina and Ag  $\beta$ '-alumina, were measured in the frequency range from 10 Hz to 100 kHz with the aid of high sensitivity, high input impedance preamplifiers. Dispersion associated with the grain boundary polarization was observed below room temperature. The frequency dependent part of the conductivity of grain interiors was seen in the four-probe spectra below 200 K. Two-probe impedance spectra were measured for samples with platinum electrodes over the frequency range 0.01 Hz to 10 MHz. The spectra were analyzed by nonlinear least-squares fitting of equivalent circuits. The circuit composed of two sections connected in series: (i) resistance  $R_{gi}$  parallel to constant phase element  $P_{gi}$ , (ii) parallel combination of resistance  $R_{gb}$ , constant phase element  $P_{gb}$  and capacitance  $C_{gb}$ , was found to be a good model of the dispersion seen in the four-probe spectra and was also part of the circuit used to simulate the two-probe spectra. The results obtained by the two-probe and four-probe methods for the resistance of grains,  $R_{gi}$ , and total resistance,  $R_t = R_{gi} + R_{gb}$ , are compared. The advantages and limitations of the two methods are discussed. © 1999 Elsevier Science B.V. All rights reserved.

**Keywords:** Impedance spectroscopy; Grain boundary polarization; Four-probe measurements; Equivalent circuit

**Materials:** NASICON ( $\text{Na}_3\text{Zr}_2\text{Si}_2\text{PO}_{12}$ ); Na  $\beta$ '-alumina; Ag  $\beta$ '-alumina

---

## 1. Introduction

Impedance spectra of polycrystalline fast ionic conductors measured with two metallic electrodes exhibit dispersions associated with grain boundary polarization and with electrode polarization. It is usually assumed that the dispersion at high frequencies is associated with grain boundaries and at low frequencies with the electrode processes. In certain cases the electrode polarization may, how-

ever, be erroneously interpreted as associated with the grain boundaries or other processes occurring in the bulk of the ionic conductor.

Ac four-probe measurements made at a single frequency over a range of temperatures have been used for characterization of ionic conductors [1]. In the ac four-probe technique the voltage is measured across the bulk of the sample, ideally with negligible current passing through the two voltage electrodes, thus avoiding electrode polarization. Four-probe measurements made over a range of frequencies should allow observation of the dispersion of the conductivity of the bulk of the polycrystalline ma-

---

\*Corresponding author. Fax: + 48-22-6282-171.

E-mail address: jrdygas@mp.pw.edu.pl (J.R. Dygas)

terial, while the interface bulk/electrode should not influence the spectra.

Four-probe impedance measurements made with voltage probes connected directly to the differential input of an impedance analyzer are limited to low frequencies and low values of impedance [2,3]. The experimental limitations, associated with the low input impedance of the measuring circuit in combination with the high impedance of voltage electrodes and with high input capacitance in relation to the capacitance of the sample, have recently been discussed by Hsieh et al. [3], who pointed out the need of low input capacitance adapters. Four-electrode impedance measurements made with a four-terminal potentiostat were also limited to systems of low resistance [4] and exhibited artifacts at high frequencies for liquid systems [5]. Using specially designed preamplifiers with high input impedance and active shielding for voltage leads in the sample holder we were able to shift the instrumental limits considerably [6].

The four-probe impedance spectra of polycrystalline yttria stabilized zirconia, measured with voltage electrodes connected to the input of the impedance analyzer, failed to resolve the grain boundary polarization [3]. Spectra measured with the aid of the newly developed preamplifiers clearly exhibited grain boundary polarization in the case of polycrystalline oxygen ion conductors: yttria stabilized zirconia and BICUVOX.10 ( $\text{Bi}_2\text{V}_{0.9}\text{Cu}_{0.1}\text{O}_{5.35}$ ) [6]. The values of the grain interior and the grain boundary conductivity were in agreement with the two-probe measurements.

Here we report results of a four-probe and two-probe impedance study of polycrystalline cation conductors: NASICON, Na  $\beta'$ -alumina and Ag  $\beta'$ -alumina. The purpose of this paper is to demonstrate that the dispersion of the conductivity of cation conductors, which is associated with electric polarization at the grain boundaries, can be studied by measurement over a range of frequencies of the impedance in the four electrode configuration and that the results agree with those obtained in the better established two electrode configuration. In addition, the frequency dependence of the grain conductivity arising from the hopping mechanism of the ionic transport [7] was observed in the four-probe spectra

in agreement with the two-probe spectra, the result which, according to our knowledge, has not been reported until now.

## 2. Experimental

Samples of polycrystalline NASICON ( $\text{Na}_3\text{Zr}_2\text{Si}_2\text{PO}_{12}$ ) were cut from a large pellet synthesized in 1983 [8]. Samples from the same batch have been investigated by impedance spectroscopy [8,9], neutron diffraction [9] and measurements of complex permittivity at microwave frequencies [10]. No degradation of the material was observed over the years and conductivity values obtained in this work are the same as measured with fresh samples.

Bars of polycrystalline Na  $\beta'$ -alumina were obtained from Ceramtec (USA). The material had nominal composition: 90.4%  $\text{Al}_2\text{O}_3$ , 8.85%  $\text{Na}_2\text{O}$ , 0.75%  $\text{Li}_2\text{O}$ . Samples of Ag  $\beta'$ -alumina were obtained by ion exchange in molten  $\text{AgNO}_3$  [11].

All samples were rectangular platelets (large face  $10 \times 5$  mm, thickness between 0.25 and 1 mm). The faces of the samples were polished using 2400 grit SiC paper. Platinum films serving as electrodes were deposited by dc plasma sputtering in argon. Samples for the two-probe measurement had electrodes covering either the large faces or the longer narrow faces. The electrodes were contacted by spring loaded gold plates of the sample holder [12]. Samples for the four-probe measurement had current electrodes covering the small faces and voltage electrodes in the form of two narrow (0.7 mm) strips of platinum on one large face at a distance of about 6 mm. The voltage electrodes were contacted in the sample holder by spring loaded platinum tips with actively shielded leads [6], the current electrodes were glued to platinum wires using platinum paste [7]. With the distance between centers of the voltage electrodes  $d$  and the cross section of the sample  $S$ , the geometric factor  $d/S$  was used for calculating the conductivity.

The two-probe measurements were made with the setup for measurement of large impedances, based on the Solartron 1260 Impedance Analyzer and the Keithley 428 Current Amplifier, which is capable of measuring impedance of absolute value up to the order of  $10^{13} \Omega$  at low frequencies [12]. The

frequency range was 0.01 Hz to 10 MHz, the amplitude of the ac signal was between 5 and 300 mV depending on the resistance of the sample. The temperature of the sample placed in vacuum was stabilized between 90 and 425 K using a closed cycle helium refrigeration system from CTI-Cryogenics and an analog controller DRC-91CA from Lake Shore Cryotronics. The silicon diode temperature sensor was soldered to the gold plate contacting the sample.

The instrumentation for the four-probe measurements has been described in Ref. [6]. The input impedance at the tips of the voltage probes was  $R_{in} > 10^{14} \Omega$ ,  $C_{in} < 0.2$  pF. The sensitivity of the current to voltage converter limited the absolute value of the measured impedance to maximum 10 G $\Omega$ . The ac outputs of the current and voltage amplifiers were compared by the Hewlett-Packard 3475A gain-phase meter. The amplitude of the ac signal applied to the current electrodes was adjusted between 0.1 and 10 V in order to reach a sufficient signal level between the voltage electrodes. Measurements were made in the temperature range between 160 and 720 K. The four-probe sample holder [6] was either inserted into an electric oven or placed in a Dewar flask above liquid nitrogen and heated by a resistive coil wrapped around the quartz tube, which enclosed the sample. Temperature was measured with the NiCr–Ni thermocouple and controlled by an Eurotherm 815. The sample chamber was flushed with nitrogen.

Both the two-probe and four-probe impedance spectra were analyzed by means of nonlinear least-squares fitting of equivalent circuits which were composed of resistors, capacitors and constant phase elements – *cpe* with the aid of program FIRDAC [8]. The complex admittance of a *cpe* was expressed as a function of the angular frequency  $\omega$  as:  $Y(\omega) = A(j\omega)^{1-N}$ , thus with the exponent parameter  $N = 0$  the *cpe* corresponded to ideal capacitance, with  $N = 1$  to resistance.

Corrections expressed as a polynomial of frequency were applied during fitting in order to reproduce distortions introduced by the instrumentation. This procedure of correction, developed for the nonideal behavior of current to voltage converters in the two-probe measurements [12], proved to

be applicable for the high frequency distortions in the four-probe measurements, when the frequency was kept below the range of gain peaking of the amplifiers.

### 3. Results and discussion

The four-probe spectra were successfully measured in the temperature range which extended down to about 160 K, the lower bound being imposed by: (i) the dc saturation of the voltage amplifiers due to the input bias current when impedance of the voltage electrodes was too high, (ii) sensitivity of the current amplifier.

The impedance spectra of the three studied fast ionic conductors exhibited similar dependence on temperature. The examples of the two-probe and four-probe impedance spectra were selected from a different temperature range for each of the materials. They are presented in Figs. 1–5 in three kinds of plots: (a) the Bode-type plot of the phase angle and the logarithm of the absolute value of impedance versus the logarithm of frequency, (b) the complex plane plot of impedance, (c) the complex plane plot of admittance. The Bode plots contain all data points taken into account during fitting of the equivalent circuit. In the complex plane plots the two-probe spectra are limited to the frequency range of the accompanying four-probe spectrum. The data measured near the high frequency limit of a given range are corrected for instrumental distortions according to the polynomial formula described in Ref. [12] (except for Fig. 5a which presents data as measured).

An example four-probe impedance spectrum at low temperature 168.5 K is given in Fig. 1 for Na  $\beta''$ -alumina sample with geometric factor  $d/S = 3050$  m<sup>-1</sup>. The maximum of the phase angle near 20 Hz indicates the frequency range of dispersion associated with grain boundary polarization. Only part of the corresponding semicircle in the complex impedance plot is within the measured frequency range, thus the low frequency intercept with the real axis, which gives the total resistance, can be obtained from the plot solely by extrapolation. The increase of the phase angle at frequencies above 600 Hz, which appears as the inclined spur in the complex admitt-

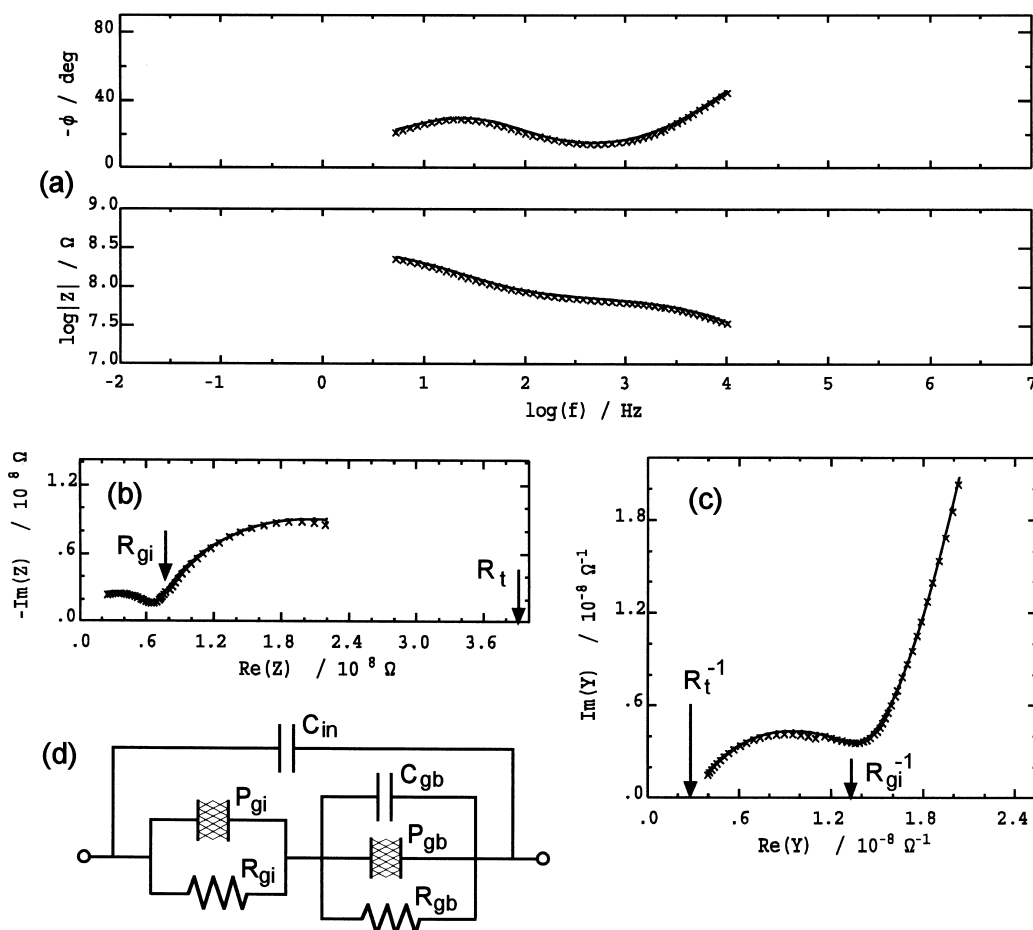


Fig. 1. Impedance of polycrystalline Na  $\beta''$ -alumina measured at 168.5 K by the four-probe technique: (a) phase and absolute value of impedance versus frequency, (b) complex plane plot of impedance, (c) complex plane plot of admittance. Symbols mark measured values, lines the fitted impedance of the equivalent circuit shown in (d). Cross-hatched capacitors denote constant phase elements. Arrows in (b) and (c) mark the estimated values of grain interior,  $R_{gi}$ , and total,  $R_t$ , resistance.

ance plot, indicates the frequency dependence of the ionic conductivity. The two-probe impedance spectrum of another sample of Na  $\beta''$ -alumina ( $d/S = 1420 \text{ m}^{-1}$ ) measured at 168 K is presented in Fig. 2. The maximum of the phase angle at about 30 Hz is obscured by the increase of phase angle due to the dominating impedance of blocking electrodes. The complex impedance plot has no minimum indicating the total resistance, only a deflection from an arc to a low frequency spur. The onset of the frequency dependence of the ionic conductivity is at about 1000 Hz.

Examples of the impedance of Ag  $\beta''$ -alumina

measured at 242 K are given in Figs. 3 and 4. The geometric factor was  $d/S = 2770 \text{ m}^{-1}$  for the sample used for the four-probe measurements and  $d/S = 8.2 \text{ m}^{-1}$  for the sample measured by the two-probe technique. The maximum of phase angle associated with the grain boundary polarization is at about 4 kHz. The phase of the four-probe impedance approaches zero at low frequencies, the intercept with the real axis in complex plane plots clearly indicates the value of the total resistance. The resistance of grain interiors is not well defined in the four-probe data – the phase angle does not approach zero at high frequencies. The extrapolation of the arcs in

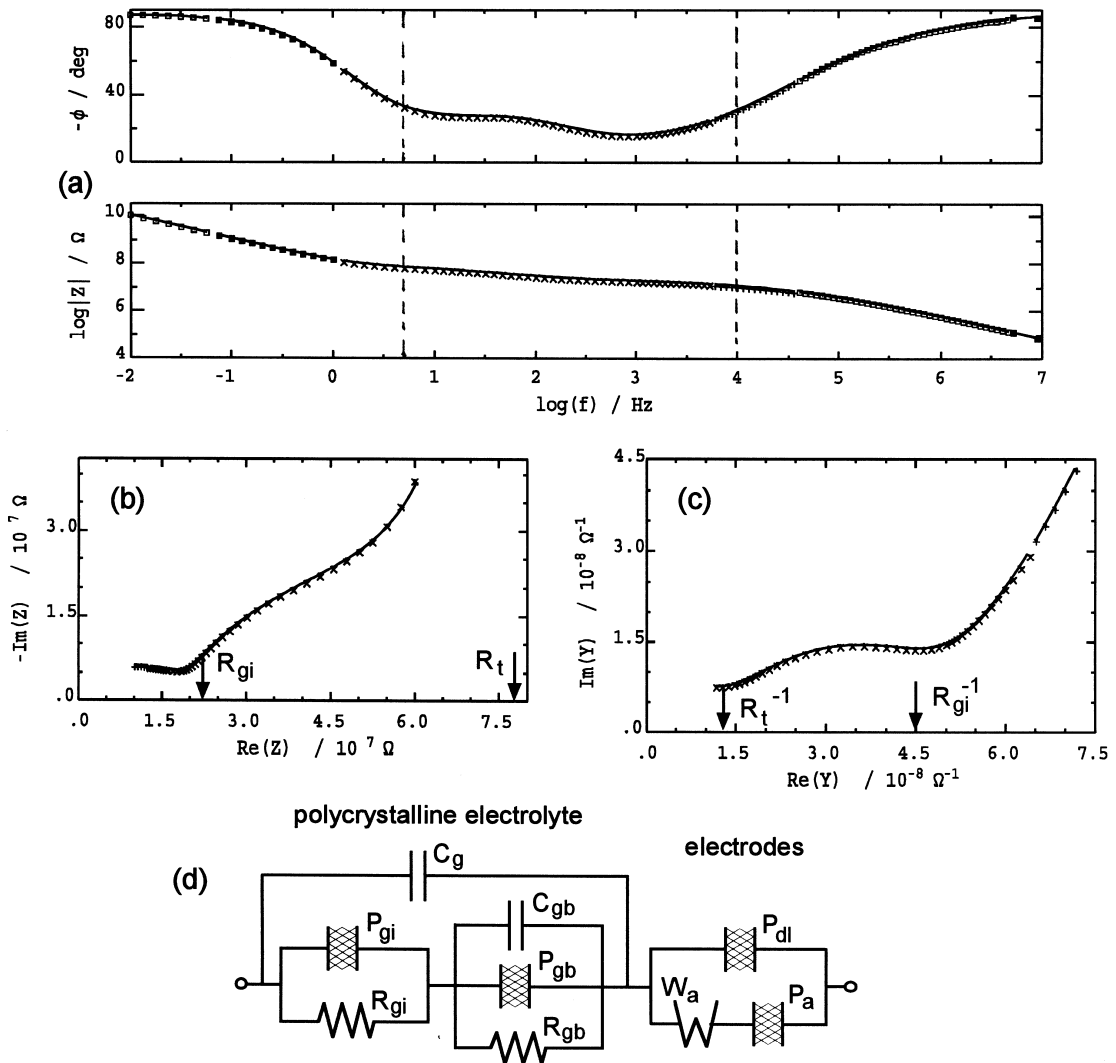


Fig. 2. Impedance of polycrystalline Na  $\beta''$ -alumina measured at 168 K by the two-probe technique: (a) phase and absolute value of impedance versus frequency, (b) complex plane plot of impedance, (c) complex plane plot of admittance. Frequency range in (b) and (c) is from 5 Hz to 10 kHz. Symbols mark measured values, lines the fitted impedance of the equivalent circuit shown in (d). Arrows in (b) and (c) mark the estimated values of grain interior,  $R_{gi}$ , and total,  $R_t$ , resistance.

complex plane plots – Fig. 3b and c – to the high frequency intercept is ambiguous. The two-probe spectrum in Fig. 4b and c allows better determination of the grain interior resistance. The impedance of blocking electrodes dominates the two-probe spectrum at low frequencies and does not allow straightforward determination of the total resistance.

The impedance spectra of NASICON presented in Fig. 5 were measured above room temperature at

about 320 K. The dispersion associated with grain boundary polarization falls above the frequency range covered by the four-probe technique – the maximum of phase angle at about 1.6 MHz is seen in the two-probe spectrum in Fig. 5b. The four-probe impedance spectrum is essentially flat. The slight increase of phase and decrease of absolute value at frequencies above 10 kHz, seen in Fig. 5a, is caused by instrumental factors. Thus no dispersion of the

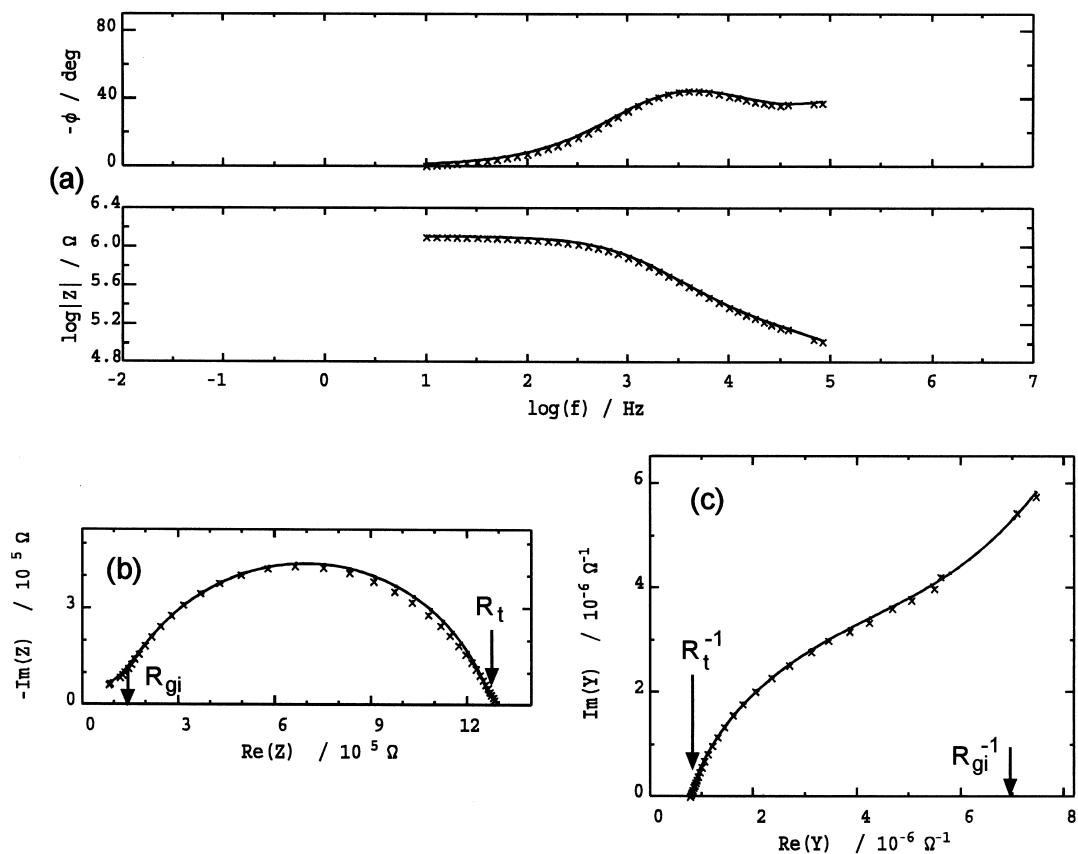


Fig. 3. Impedance of polycrystalline Ag  $\beta''$ -alumina measured at 242 K by the four-probe technique: (a) phase and absolute value of impedance versus frequency, (b) complex plane plot of impedance, (c) complex plane plot of admittance. Symbols mark measured values, lines the fitted impedance of the equivalent circuit of Fig. 1d.

bulk impedance is observed by the four-probe technique, at least below 10 kHz. On the contrary, a distinct maximum of phase is seen in the two-probe spectrum near 700 Hz (Fig. 5b). By extrapolation to the real axis of the arc present in the complex plane plots, limited to the frequency range from 10 Hz to 100 kHz (Fig. 5c and d), one may extract two values of resistance. These two values may be erroneously interpreted as the total  $R_t$  and the grain interior  $R_{gi}$  resistance. In reality, the total resistance of the polycrystalline ionic conductor corresponds in this case to the high frequency intercept with the real axis. The arc in the complex plane plots of the two-probe impedance is associated with the interface platinum electrode/NASICON, which does not behave at elevated temperature as a simple blocking electrode. If the four-probe measurements were not

available, the association of the dispersion seen in the two-probe spectrum below 10 kHz with the electrode impedance and not with the bulk of the polycrystalline NASICON could be proved by examination of scaling with the geometric factor of the parameters of an appropriate equivalent circuit evaluated for samples of different length [13].

Various forms of equivalent circuit were tested by means of nonlinear least-squares fitting in order to find the best model of the measured impedance. Fits of similar quality were obtained with different circuits. Comparison between results obtained for the two-probe and the four-probe spectra was used as a criterion to select the equivalent circuit. It has to be pointed out that, since the electrode polarization overlaps in frequency with the grain boundary polarization in the two-probe spectra, particularly in

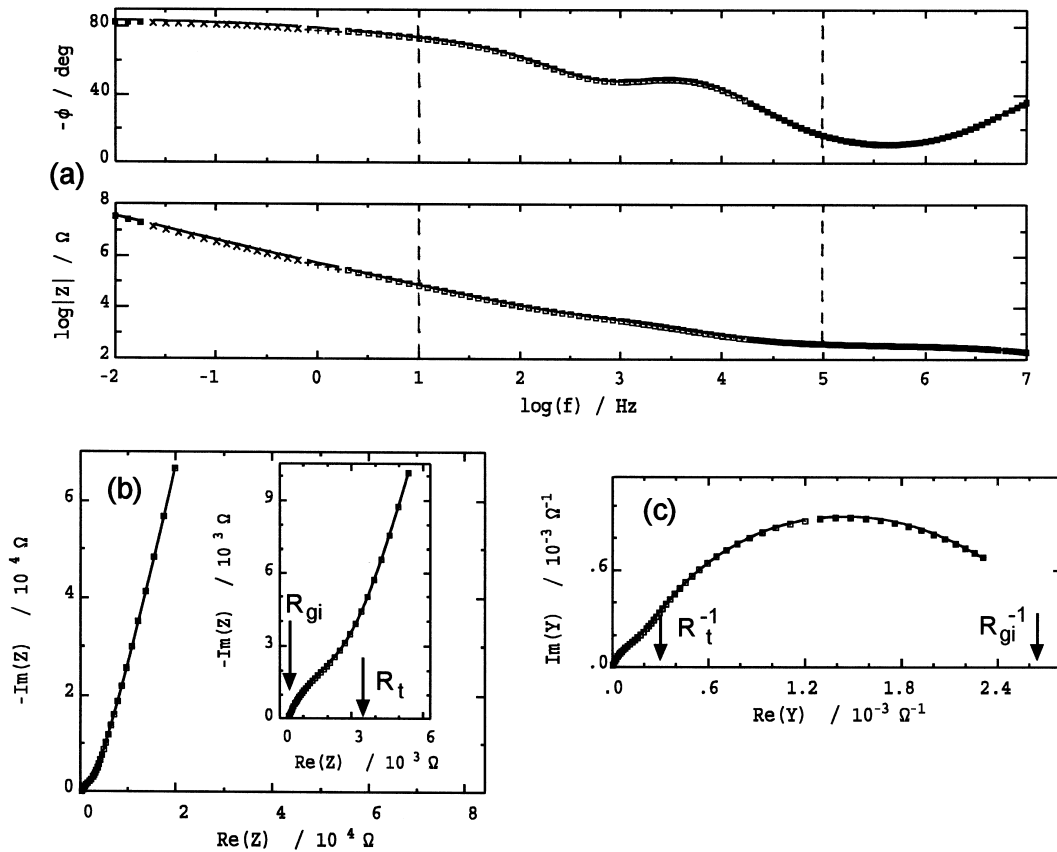


Fig. 4. Impedance of polycrystalline Ag  $\beta''$ -alumina measured at 242 K by the two-probe technique: (a) phase and absolute value of impedance versus frequency, (b) complex plane plot of impedance, (c) complex plane plot of admittance. Frequency range in (b) and (c) is from 10 Hz to 100 kHz. Symbols mark measured values, lines the fitted impedance of the equivalent circuit of Fig. 2d.

the case of Na  $\beta''$ -alumina, the fitted values of the grain boundary resistance,  $R_{gb}$ , and the total resistance,  $R_t = R_{gb} + R_{gi}$ , depend on the form of the circuit used to model the electrode polarization. The resistance of grain interiors  $R_{gi}$  is estimated from the two-probe spectra with much less ambiguity, as long as the frequency of the dispersion associated with grain boundaries is well below the upper frequency ( $10^7$  Hz) of the measured spectra. Since the upper frequency of the four-probe spectra is  $10^5$  Hz, and data measured above  $10^4$  Hz were distorted due to the limited bandwidth of the amplifiers, the values of  $R_{gi}$  obtained from the four-probe spectra are less accurate and depend on the form of the equivalent circuit. The agreement between the values of grain interior conductivity obtained by the two methods was improved by using the same equivalent circuit to

fit the two-probe and four-probe impedance spectra and by fixing exponents of the *cpe* at values obtained from the two-probe spectra.

The circuits presented in Fig. 1d and Fig. 2d were finally selected as giving the best agreement between the conductivity values obtained from the four-probe and the two-probe measurements. The *cpe*  $P_{gi}$  reproduces the frequency dependent part of the ionic conductivity of grain interiors. The polarization at grain boundaries is modeled by the *cpe*  $P_{gb}$  and the capacitor  $C_{gb}$ . Using  $C_{gb}$  parallel to  $P_{gb}$  with the exponent  $N_{gb} = 0.5$  resulted in significant improvement of fit in the case of Na  $\beta''$ -alumina. The spectra of the other two ionic conductors were simulated using circuit without  $C_{gb}$ , while the values of the *cpe* exponent were  $N_{gb} \cong 0.2$ . The equivalent circuit used to simulate the four-probe spectra, Fig. 1d, has the

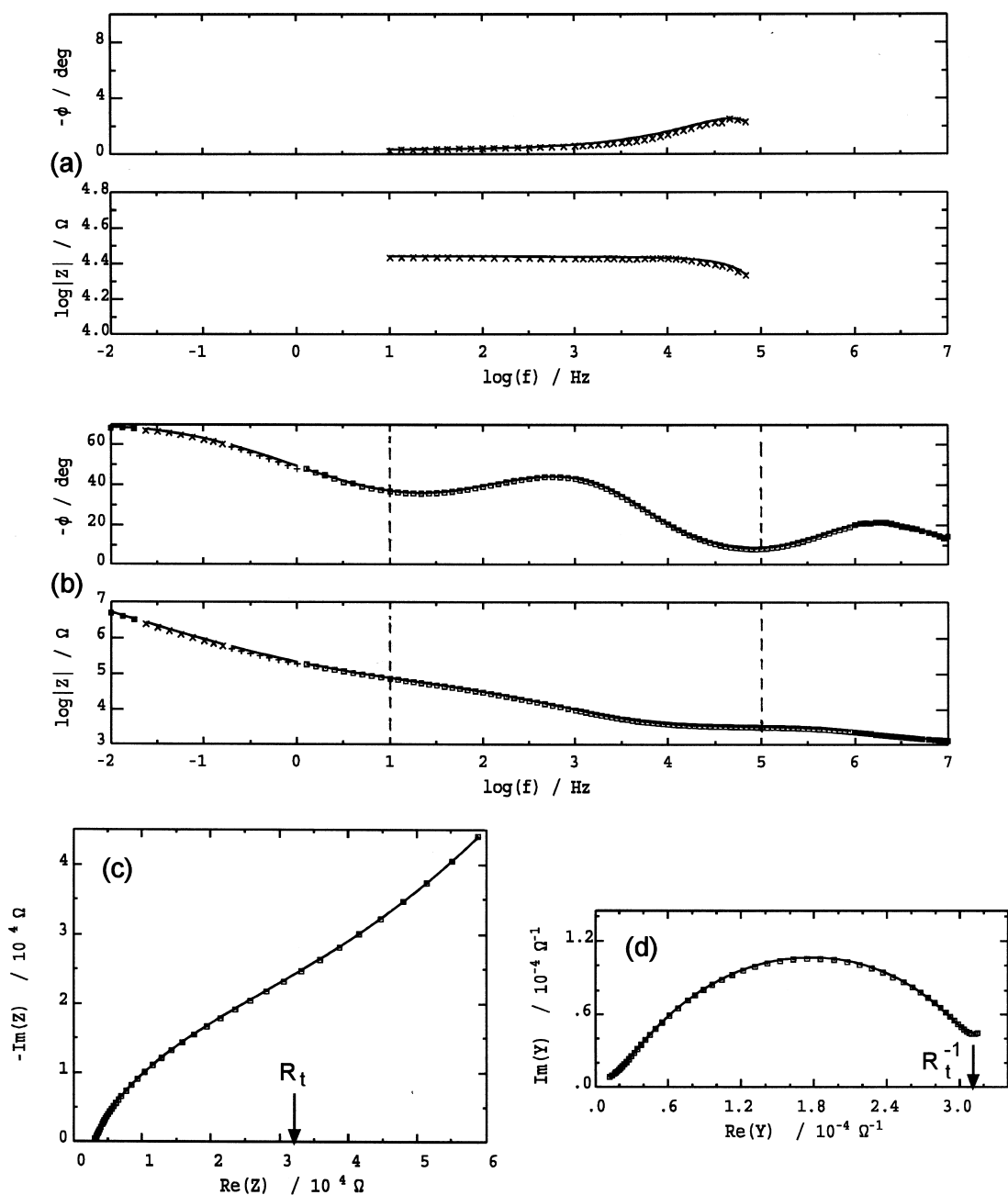


Fig. 5. Impedance of polycrystalline NASICON: (a) measured at 321 K by the four-probe technique; (b), (c) and (d) measured at 319 K by the two-probe technique. Frequency range in (c) and (d) is from 10 Hz to 100 kHz.

same form as this part of the circuit used to simulate the two-probe spectra which represents the impedance of the polycrystalline electrolyte.

The part of the circuit in Fig. 2d, which models

the electrode impedance consists of a *cpe*  $P_{al}$ , which represents the double layer capacitance, and a parallel branch of a Warburg element  $W_a$  in series with a *cpe*  $P_a$ , which can be interpreted as a diffusion

controlled adsorption. The equivalent circuit of Fig. 2d fitted well the impedance measured at low temperatures. At elevated temperatures a more complex circuit was needed to model the electrode impedance, particularly in the case of NASICON, as evidenced by spectra shown in Fig. 5. In this case, the equivalent circuit included additionally a resistance and *cpe* elements in the part modeling the interface Pt/NASICON. The physical interpretation of such an equivalent circuit is not clear. It is not the purpose of this paper to discuss the properties of platinum electrodes on the cationic conductors, which seem to be much more complicated than expected for a simple blocking electrode.

The temperature dependence of the grain interior conductivity,  $\sigma_{gi} = d/(S \cdot R_{gi})$ , and the total conductivity,  $\sigma_t = d/[S \cdot (R_{gi} + R_{gb})]$ , evaluated from the four-probe and two-probe impedance spectra is presented in Figs. 6–8. The range of temperature in which it was possible to evaluate the grain interior conductivity by the four-probe technique was somewhat different for the three studied materials. For Na  $\beta''$ -alumina it was below 280 K, for Ag  $\beta''$ -alumina below 305 K, and for NASICON below 260 K. The two-probe technique allowed evaluation of the grain interior conductivity in a broader temperature range. The agreement between the values of grain interior conductivity obtained by the two techniques is good in the upper part of the temperature range in which evaluation by the four-probe technique was possible.

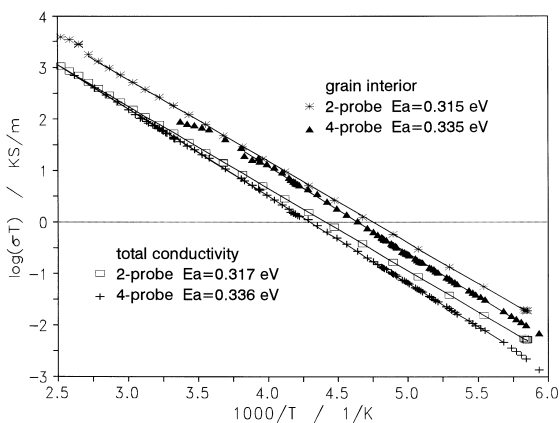


Fig. 6. Temperature dependence of the grain interior and total conductivity of Na  $\beta''$ -alumina measured by the four-probe technique and by the two-probe technique.

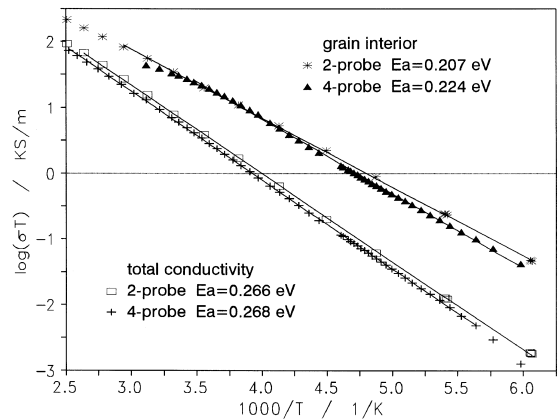


Fig. 7. Temperature dependence of the grain interior and total conductivity of Ag  $\beta''$ -alumina measured by the four-probe technique and by the two-probe technique.

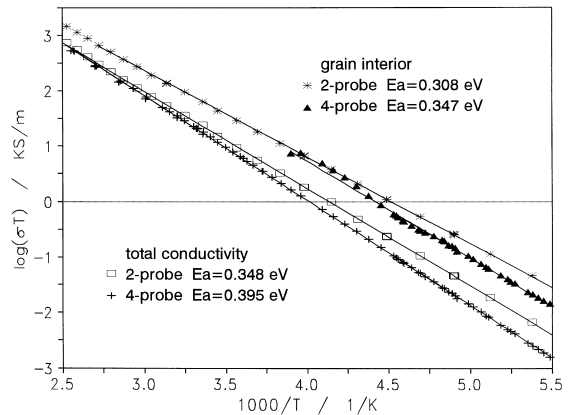


Fig. 8. Temperature dependence of the grain interior and total conductivity of NASICON measured by the four-probe technique and by the two-probe technique.

The relative difference between the two sets of values increases with decreasing temperature, the conductivity values obtained by the four-probe technique are lower. The agreement is the best in the case of Ag  $\beta''$ -alumina and the worse in the case of NASICON, but the ratio of the values obtained by the two techniques does not exceed the factor 2.

The values of the total conductivity agree well for all samples around and above the room temperature, but values obtained by the four-probe technique are systematically lower. The ratio of the total conductivity value from the two-probe to the value from the four-probe increases with decreasing tempera-

ture. In the case of Ag  $\beta''$ -alumina the ratio of the two values remains within a factor of 1.5 down to 170 K, in the case of NASICON it is above 2.5 at temperatures below 180 K.

Values of activation energy  $E_a$ , obtained by fitting the formula  $\sigma T = \sigma_0 \exp(-E_a/kT)$  to the temperature dependence of conductivity, are listed in Figs. 6–8. The values of activation energy obtained from the four-probe measurements are larger than the corresponding values from the two-probe measurements, both for the total conductivity and the conductivity of grain interiors. The difference is within 0.02 eV for the two isomorphs of  $\beta''$ -alumina, and about 0.04 eV for NASICON. Only in the case of Ag  $\beta''$ -alumina do the values of activation energy of the total conductivity agree within the estimation error.

The difference between the total conductivity values obtained by the two-probe and four-probe techniques is not larger than reported in the previous study which compared the two-probe impedance spectroscopy with the four-probe measurement at a single frequency [14]. The reason for the remaining discrepancy is not fully understood. Various factors have been considered:

- (1) systematic error in measurement of temperature;
- (2) voltage divider between input impedance of voltage amplifiers and impedance of the voltage electrodes, discussed by Hsieh et al. [3];
- (3) influence of voltage electrodes on distribution of current in the sample;
- (4) cross-talk between the differential mode and common mode of the voltage amplifier.

Cross-calibration of temperature meters did not confirm factor (1). The voltage divider – factor (2) – would typically act to decrease the measured voltage; thus the values of resistance obtained by the four-probe technique should be lower than actual. The opposite effect is only conceivable in the case of strongly asymmetric voltage electrodes [3], which is unlikely when identical sputtered platinum films were used as electrodes. Rough estimation shows that the effect of a finite width of voltage electrodes should not introduce relative error of the measured impedance larger than the ratio of the width of electrodes to the distance between them, which was less than 15%. Since the difference between the two-probe and four-probe data was larger, factor (3)

cannot explain it. The cross-talk of the common mode – factor (4) – may be a plausible explanation since the total voltage applied to the sample with blocking electrodes is several orders of magnitude larger than the difference of voltage between the two voltage probes, as can be deduced from comparison of the absolute values of impedance in the two-probe and four-probe spectra at low frequencies. The dc polarization present between the voltage electrodes as an effect of finite input bias current of the amplifier may enhance the effect of cross-talk.

In the case of the oxide ion conductor BICUVOX [15], the agreement between the conductivity values obtained by the four-probe and two-probe measurements was better than in the present study of cation conductors. This is likely to be related to different properties of platinum electrodes with oxide ion and cation conductors. The fact that the same digital frequency response analyzer was used to measure the ratio of current to voltage signals in the four-probe and two-probe measurements on BICUVOX [15] might have been essential for obtaining the better agreement.

#### 4. Conclusions

Below room temperature, dispersion of the conductivity of polycrystalline cation conductors was observed in four-probe impedance measured from 10 Hz to 100 kHz. The same dispersion was seen in two-probe impedance spectra. The equivalent circuit, which reproduced the grain boundary polarization and the frequency dependence of the conductivity of grain interiors of polycrystalline cation conductors, was fitted to the four-probe spectra and was part of the circuit used to model the two-probe spectra. The values of the circuit parameters obtained by analysis of two-probe and four-probe spectra agree roughly.

The two-probe impedance spectra extend to high frequencies, which is advantageous for determination of the conductivity of grain interiors, but at low frequencies are dominated by the impedance of blocking electrodes. The four-probe impedance spectra do not contain contributions from the current electrodes and allow measurement of the total conductivity down to low frequencies. Comparison of

results obtained by the two techniques is crucial for avoiding erroneous interpretation of the impedance spectra.

## References

- [1] P. Linhardt, M. Maly-Schreiber, M.W. Breiter, in: F.W. Poulsen, N.H. Andersen, K. Clausen, S. Skaarup, O.T. Sorensen (Eds.), *Proc. 6th Int. Symp. Metallurgy and Materials Science*, RISO National Laboratory, Roskilde, Denmark, 1985, p. 475.
- [2] J.J. Bentzen, N.H. Andersen, F.W. Poulsen, O.T. Sorensen, R. Schram, *Solid State Ionics* 28–30 (1988) 550.
- [3] G. Hsieh, S.J. Ford, T.O. Mason, L.R. Pederson, *Solid State Ionics* 100 (1997) 297.
- [4] B.D. Cahan, J.S. Wainright, *J. Electrochem. Soc.* 140 (1993) L185.
- [5] M.C. Wiles, D.J. Schiffrin, T.J. VanderNoot, A.F. Silva, *J. Electroanal. Chem.* 278 (1990) 151.
- [6] G. Fafilek, M.W. Breiter, *J. Electroanal. Chem.* 430 (1997) 269.
- [7] K. Funke, *Prog. Solid St. Chem.* 22 (1993) 111.
- [8] J.R. Dygas, Ph.D. Thesis, Northwestern University, Evanston, 1986.
- [9] W.H. Baur, J.R. Dygas, D.H. Whitmore, J. Faber, *Solid State Ionics* 18–19 (1986) 935.
- [10] J.R. Dygas, M.E. Brodwin, *Solid State Ionics* 18–19 (1986) 981.
- [11] M. Maly-Schreiber, P. Linhardt, M.W. Breiter, *Solid State Ionics* 23 (1987) 131.
- [12] J.R. Dygas, M.W. Breiter, *Electrochim. Acta* 41 (1996) 993.
- [13] J.R. Dygas, in *Proc. 5th National Symp. Przewodniki szybkich jonow*, Oficyna Wyd. Politechniki Warszawskiej, Warszawa 1995, p. 121.
- [14] M.W. Breiter, H. Durakpasa, G. Dorner, P. Linhardt, *Mater. Sci. Eng.* B3 (1989) 125.
- [15] P. Kurek, G. Fafilek, *Solid State Ionics*, this volume.